Case Studies in Thermal Engineering 8 (2016) 226–235

Contents lists available at ScienceDirect

Case Studies in Thermal Engineering

journal homepage: www.elsevier.com/locate/csite

Numerical investigation on turbulent forced convection and heat transfer characteristic in a square channel with discrete combined V-baffle and V-orifice

Amnart Boonloi [a], Withada Jedsadaratanachai [b,*]

[a] Department of Mechanical Engineering Technology, College of Industrial Technology, King Mongkut's University of Technology North Bangkok, Bangkok 10800, Thailand

[b] Department of Mechanical Engineering, Faculty of Engineering, King Mongkut's Institute of Technology Ladkrabang, Bangkok 10520, Thailand

ARTICLE INFO

Article history:
Received 13 April 2016
Received in revised form
7 July 2016
Accepted 9 July 2016
Available online 12 July 2016

Keywords:
V-baffle
V-orifice
Vortex generator
Numerical study
Turbulent flow

ABSTRACT

Turbulent forced convection, heat transfer and performance improvement in a square channel with discrete combined baffles (*DCB*), which combined V-baffle and V-orifice, are investigated numerically. The influences of the flow blockage ratios (BR=0.05, 0.10 and 0.15) and V-tip directions (V-tip pointing downstream called "V-Downstream" and V-tip pointing upstream called "V-Upstream") are examined with a single pitch spacing ratio, PR=1, and attack angle, α=30°, for the Reynolds number, Re=5000–20,000. The computation results are reported in terms of flow visualizations, heat transfer characteristics, performance assessments. The results are compared with the smooth channel and the previous works. As the results, the *DCB* enhances the heat transfer rate and thermal efficiency due to the disturbance of the thermal boundary layer. The improvement of the heat transfer rate is around 2.8–6 times higher than the smooth channel depended on BR, V-tip directions and Re. In addition, the computational result reveals that the optimum thermal enhancement factor, *TEF*, is around 1.72 at BR=0.1, Re=3000 and V-Upstream.

1. Introduction

Passive technique had been used to augment heat transfer rate and thermal performance in various types of heat exchangers; fin-and-tube heat exchanger, solar air heater channel, shell-and-tube heat exchanger, etc. The main objective of the passive technique is to generate the vortex flow, longitudinal vortex flow, swirling flow, impinging flow in the heating section. These behaviors disturb the thermal boundary layer on the heat transfer surface that helps to increase the heat transfer rate and efficiency.

The numerical and experimental investigations on flow and heat transfer characteristics in heating or cooling systems installed with V-shaped turbulators had been widely reported [1–14]. The parameters such as height, attack angle, arrangement, etc., of the V-shaped turbulators were studied. The researchers found that the use of the V-shaped turbulators in the system performs higher heat transfer rate and thermal efficiency than the typical system. They also concluded that the V-shaped turbulators give higher effectiveness than the other shapes of the turbulators. The V-shaped turbulators were also combined with the orifice called "V-orifice". The installation of the V-orifice in the heat exchanger was investigated by

* Corresponding author.
E-mail address: kjwithad@kmitl.ac.th (W. Jedsadaratanachai).

http://dx.doi.org/10.1016/j.csite.2016.07.003

Nomenclature

b	baffle height, m
BR	blockage ratio, (b/H)
e	gap between baffle and duct wall, m
D_h	hydraulic diameter of the square duct, m
H	duct height, m
PR	pitch ratio, (L/H)
f	friction factor
h	convective heat transfer coefficient, $\mathrm{W\,m^{-2}\,K^{-1}}$
k	turbulent kinetic energy, ($k = \frac{1}{2}\overline{u_i' u_j'}$)
k_a	thermal conductivity of air, $\mathrm{W\,m^{-1}\,K^{-1}}$
L	periodic length (distance between baffles), m
Nu	Nusselt number
P	static pressure, Pa
Pr	Prandtl number
Re	Reynolds number, $(\rho u_0 D/\mu)$
T	temperature, K
TEF	thermal performance enhancement factor, $(Nu/Nu_0)/(f/f_0)^{1/3}$
u_i	velocity component in x_i – direction, $\mathrm{m\,s^{-1}}$
$u_{i'}$	fluctuation velocity in x_i – direction, $\mathrm{m\,s^{-1}}$
u_0	mean or uniform velocity in smooth tube, $\mathrm{m\,s^{-1}}$
x	coordinate direction

Greek letter

μ	dynamic viscosity, $\mathrm{kg\,s^{-1}\,m^{-1}}$
Γ	thermal diffusivity
ε	dissipation rate
ρ	density, $\mathrm{kg\,m^{-3}}$
α	flow attack angle

Subscript

0	smooth duct
pp	pumping power

Boonloi and Jedsadaratanachai [16]. They stated that the high pressure loss is found when installed with the V-orifice. In conclusion, the V-shaped turbulators not only increase in heat transfer rate, but also enhance pressure loss. Therefore, the modified shape and installation method, which help to reduce the pressure loss in the heating system, were investigated [15].

As the previous literature reviews, it is found that the V-shaped baffle has effectiveness higher than the other types of the vortex generators. In the current investigation, the discrete combined baffles (*DCB*), which are modified from the V-baffle [14] and V-orifice [16], are inserted in the channel heat exchanger to improve the heat transfer rate and performance. The diagonal installation of the *DCB*s in the channel heat exchanger is referred from Refs. [14,15]. The proposed *DCB*s can be readily manufactured by forming process and conveniently installed in the actual heat exchanger unit. The discrete configuration [15] is applied to the *DCB*s to decrease the pressure loss and also helps to enhance the strength of the vortex flow (increase vortex intensity). The influences of the blockage ratios (b/H, BR=0.05–0.15) and flow directions (V-Downstream and V-Upstream) are investigated for the turbulent regime, Re=3000–20,000. The pitch ratio and flow attack angle of the *DCB* are fixed at 1 and 30°, respectively. The numerical method is selected to explain the behaviors of the presented problem. Knowledge of the mechanisms on flow and heat transfer characteristics is a powerful tool for further improvement of the heat exchanger.

2. Computational configuration

The configurations of the V-baffle, V-orifice, full combined baffle and discrete combined baffle are reported in the Fig. 1a, b, c and d, respectively. The square channel with the *DCB*s and the computational domain are depicted as Fig. 2a. The *DCB* is designed from the combination between V-baffle and V-shaped orifice. The discrete configuration (like staggered arrangement) is used to reduce the pressure loss in the heating section. The square channel height, H, is set around 0.05 m. The *DCB*s inserted in the square channel heat exchanger with gap ratio, e/H, of 0.01. The effects of the blockage ratios (b/H=0.05. 0.10 and 0.15), and flow directions (V-Downstream and V-Upstream) are investigated for the Reynolds numbers, Re=3000–20,000, with a single pitch ratio (P/H) of 1 and flow attack angle of 30°. The grid resolution on the square channel walls is presented in Fig. 2b.

3. Mathematical foundation

The incompressible turbulent flow with steady operation in three dimensions and heat transfer characteristic in the square duct agree governed by continuity, Navier-Stokes and energy equations.

The realizable k-ε turbulent model with enhanced wall treatment is used to solve the present problem.

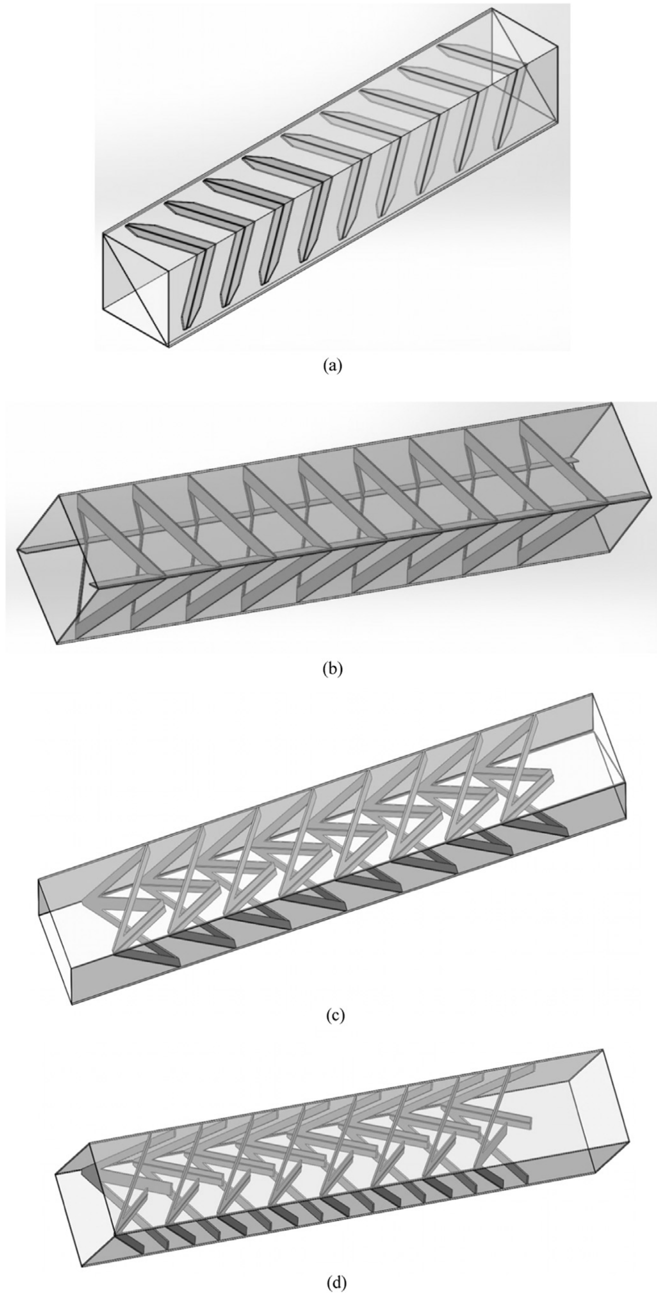

Fig. 1. Square channel heat exchanger inserted with (a) V-baffle, (b) V-orifice, (c) full combined baffle and (d) discrete combined baffle.

$$\frac{\partial}{\partial t}(\rho k) + \frac{\partial}{\partial x_j}(\rho k u_j) = \frac{\partial}{\partial x_j}\left[\left(\mu + \frac{\mu_t}{\sigma_k}\right)\frac{\partial k}{\partial x_j}\right] + G_k + G_b - \rho\varepsilon - Y_M + S_k \tag{1}$$

and

$$\frac{\partial}{\partial t}(\rho\varepsilon) + \frac{\partial}{\partial x_j}(\rho\varepsilon u_j) = \frac{\partial}{\partial x_j}\left[\left(\mu + \frac{\mu_t}{\sigma_\varepsilon}\right)\frac{\partial\varepsilon}{\partial x_j}\right] + \rho C_1 S\varepsilon - \rho C_2\frac{\varepsilon^2}{k + \sqrt{\upsilon\varepsilon}} + C_{1\varepsilon}\frac{\varepsilon}{k}C_{3\varepsilon}G_b + S_\varepsilon \tag{2}$$

where

$$C_1 = \max\left[0.43, \frac{\eta}{\eta + 5}\right], \eta = S\frac{k}{\varepsilon}, S = \sqrt{2S_{ij}S_{ij}} \tag{3}$$

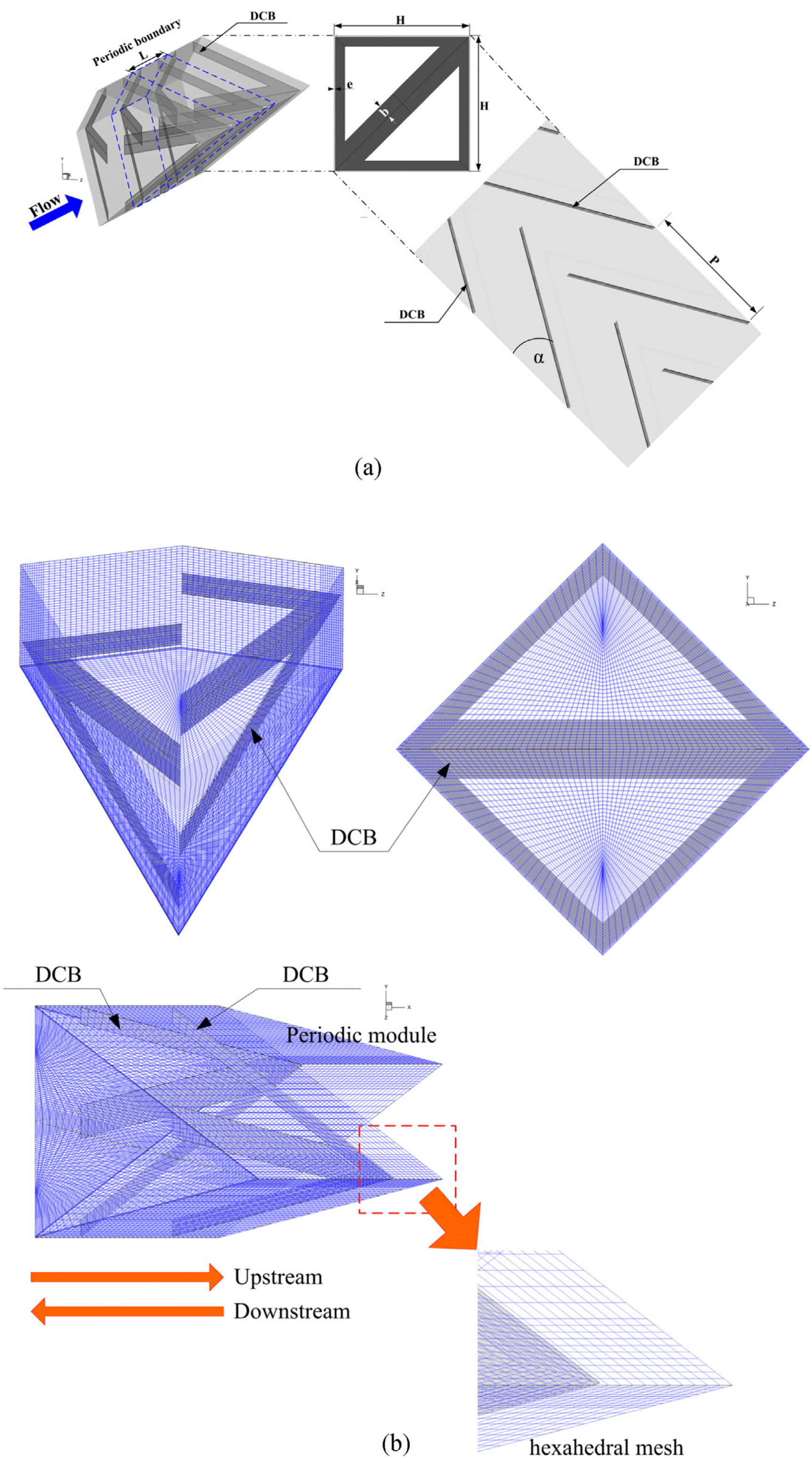

Fig. 2. (a) Square channel with *DCB*s and the computational domain and (b) mesh resolution of the square channel walls.

the constants in the model are given as follows:

$$C_{1\varepsilon} = 1.44,\ C_2 = 1.9,\ \sigma_k = 1.0,\ \sigma_\varepsilon = 1.2 \tag{4}$$

The QUICK numerical scheme is selected for all governing equations, decoupling with the SIMPLE algorithm using a finite volume method with FLUENT code. The solutions are measured to be converged when the normalized residual are less than 10^{-9} and 10^{-5} for the energy equation and the other variables, respectively.

The main parameters for the current investigation are Reynolds number (*Re*), friction factor (*f*), Nusselt number (*Nu*) and thermal enhancement factor (*TEF*).

The Reynolds number is calculated from Eq. (5).

$$\mathrm{Re} = \frac{\rho u_0 D_h}{\mu} \tag{5}$$

ρ, μ and u_0 are density, viscosity and inlet velocity of the fluid, respectively, while D_h is the hydraulic diameter of the square channel.

The friction factor is defined as

$$f = \frac{(\Delta P/L)D_h}{2\rho \bar{u}^2} \tag{6}$$

ΔP is the pressure drop across the periodic module, L, and u is mean flow velocity.

The local Nusselt number is computed by

$$Nu_x = \frac{h_x D_h}{k} \tag{7}$$

h_x is local heat transfer coefficient based on bulk temperature and k is thermal conductivity of the air.

The average Nusselt number can be printed by

$$Nu = \frac{1}{A}\int Nu_x dA \tag{8}$$

where, A is heat transfer area of the square channel heat exchanger.

Thermal performance enhancement factor (*TEF*) is defined as the ratio of the heat transfer coefficient of an augmented surface, h to that of a smooth surface, h_0, under the constant pumping power condition. The *TEF* can be expressed as follow;

$$TEF = \left.\frac{h}{h_0}\right|_{pp} = \left.\frac{Nu}{Nu_0}\right|_{pp} = \left(\frac{Nu}{Nu_0}\right)\Big/\left(\frac{f}{f_0}\right)^{1/3} \tag{9}$$

The f_0 and Nu_0 are the friction factor and the Nusselt number of the smooth tube, respectively.

4. Boundary condition and assumption

No-slip wall condition is used for all sides of the channel heat exchanger and *DCBs*. Constant heat flux around 600 W/m^2 is applied to the channel walls, while the baffles are set as an adiabatic wall condition (insulator). The air ($Pr=0.7$) as test fluid with constant properties at 300 K flows into the channel heat exchanger. The periodic condition is applied for inlet and outlet of the computational domain. The flow and heat transfer of the domain are developed under steady state. The fluid flow is turbulent and incompressible. The body force, viscous dissipation, natural convection and radiation heat transfer are ignored.

5. Numerical result and discussion

5.1. Numerical validation

The validations of the computational domain are separated into three parts; grid independence, validation with the smooth channel and validation with the experimental result. The hexahedral mesh is selected for the present computational domain. The grid independence is done by compared nine sets of the grid cells (42000, 62700, 81600, 127500, 187200, 232400, 352000, 418500 and 619400) on the Nusselt number and friction factor for the *DCB* with $BR=0.1$, $PR=1$ and $\alpha=30^{o}$. The grid cell of 232400 performs around 0.74% and 0.54% deviation for the Nusselt number and friction factor, respectively, in compared with 619400 cells. Therefore, the grid of 232400 is selected for all cases.

The validations of the Nusselt number and friction factor for the smooth channel are done. The turbulent models (Realizable k-ε and *SST* k-ω models) are also compared in this section. The Realizable k-ε provides the lowest relative errors

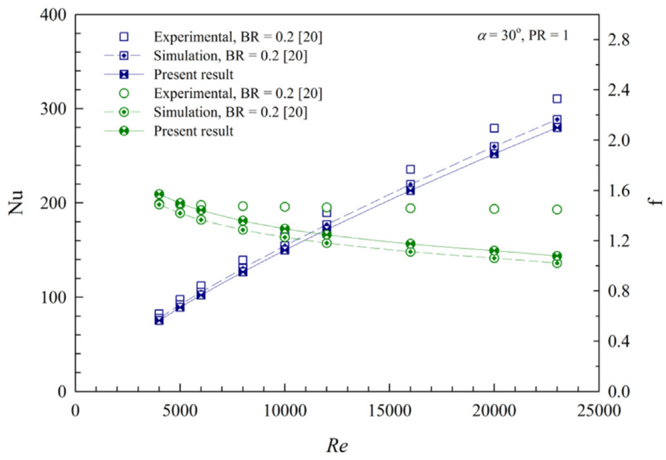

Fig. 3. Validation with experimental results.

around 4.27% and 5.4%, respectively, for the Nusselt number and friction factor when compared with the Dittus-Boelter and Blasius correlations [18].

Fig. 3 reports the comparison between the values of the previous work [19] and the present work on the Nusselt number

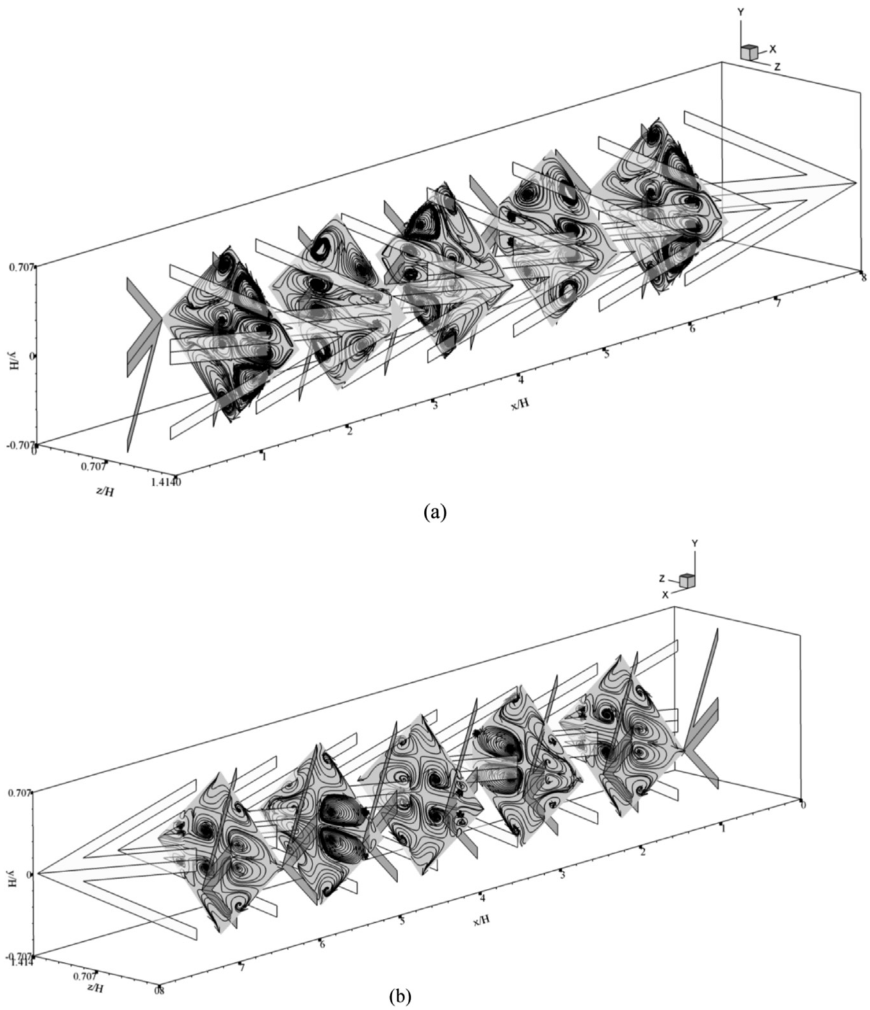

Fig. 4. Streamlines in transverse planes for the square channel with *DCB*s at $BR=0.1$ and $Re=3000$ for (a) V-Upstream and (b) V-Downstream.

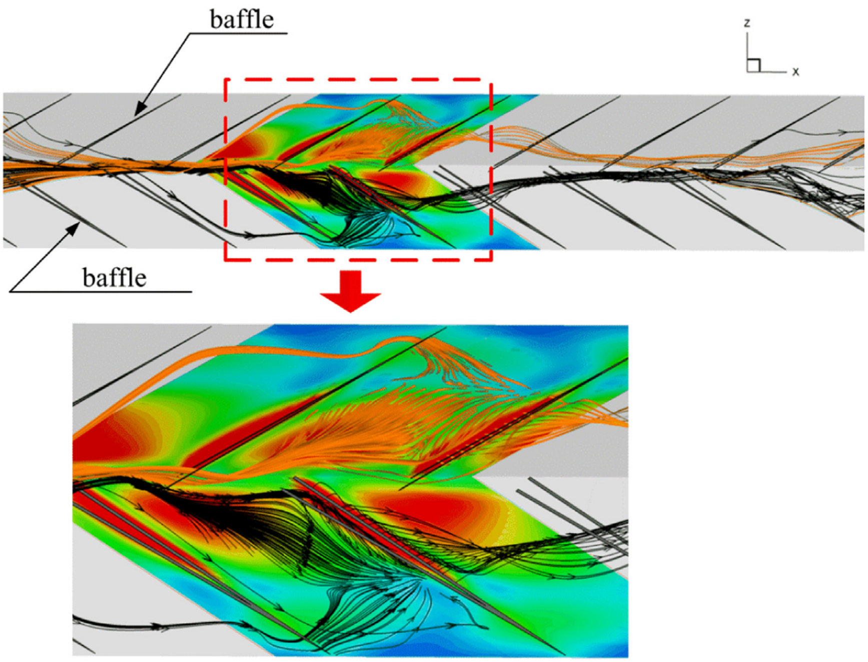

Fig. 5. Impinging flow on the square channel walls for V-Upstream at $BR=0.1$, $Re=3000$.

and friction factor. The current results are found in good agreement with the previous results on both the heat transfer rate and friction loss. Therefore, it can be concluded that the computational domain has reliable to predict the heat transfer and flow structure in the channel heat exchanger.

5.2. Flow pattern and heat transfer behavior

Fig. 4a and b display the streamlines in transverse planes of the *DCB* in the channel with $BR=1$ and $Re=3000$ for V-Upstream and V-Downstream, respectively. It is found that the *DCB* can create eight small vortices through the channel. The positions of the vortex cores for both cases are found similarly, but in an opposite direction. The vortex flow helps to improve fluid mixing in the channel. The use of the *DCB* in the heating section gives the number of the vortices higher than the inclines baffle [15], V-baffle [14] and orifice [16]. The enhancement of the vortices leads to a better distribution of the local Nusselt number on the channel walls, but the strength of each vortex may decrease.

The plots of the impinging flow on the channel wall with the local Nusselt number distributions are presented in Fig. 5 for V-Upstream case at $BR=0.1$ and $Re=3000$. As the figure, the V-Upstream produces the impinging flow on the channel

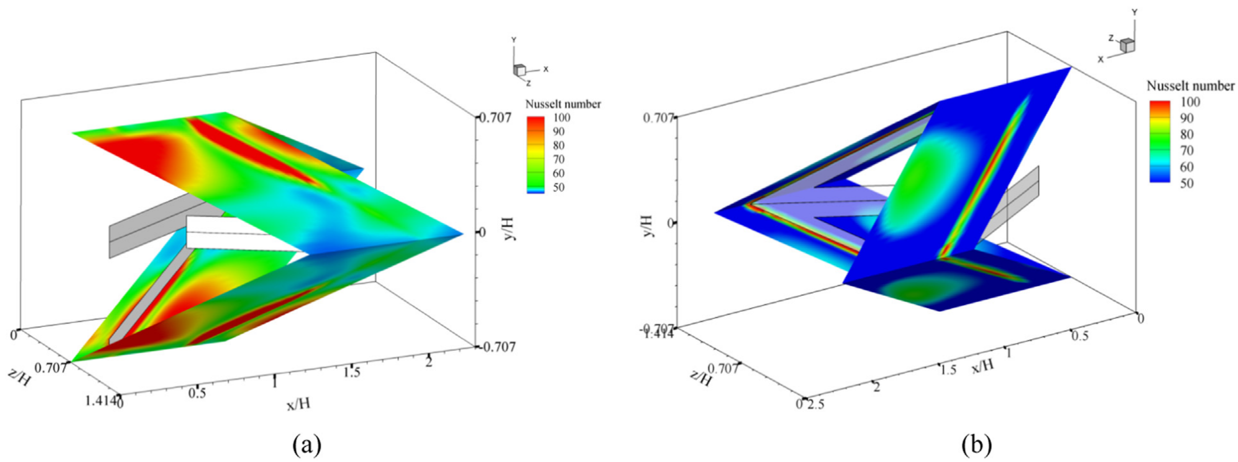

Fig. 6. Local Nusselt number distributions in transverse planes for the square channel with *DCB*s at $BR=0.1$ and $Re=3000$ for (a) V-Upstream and (b) V-Downstream.

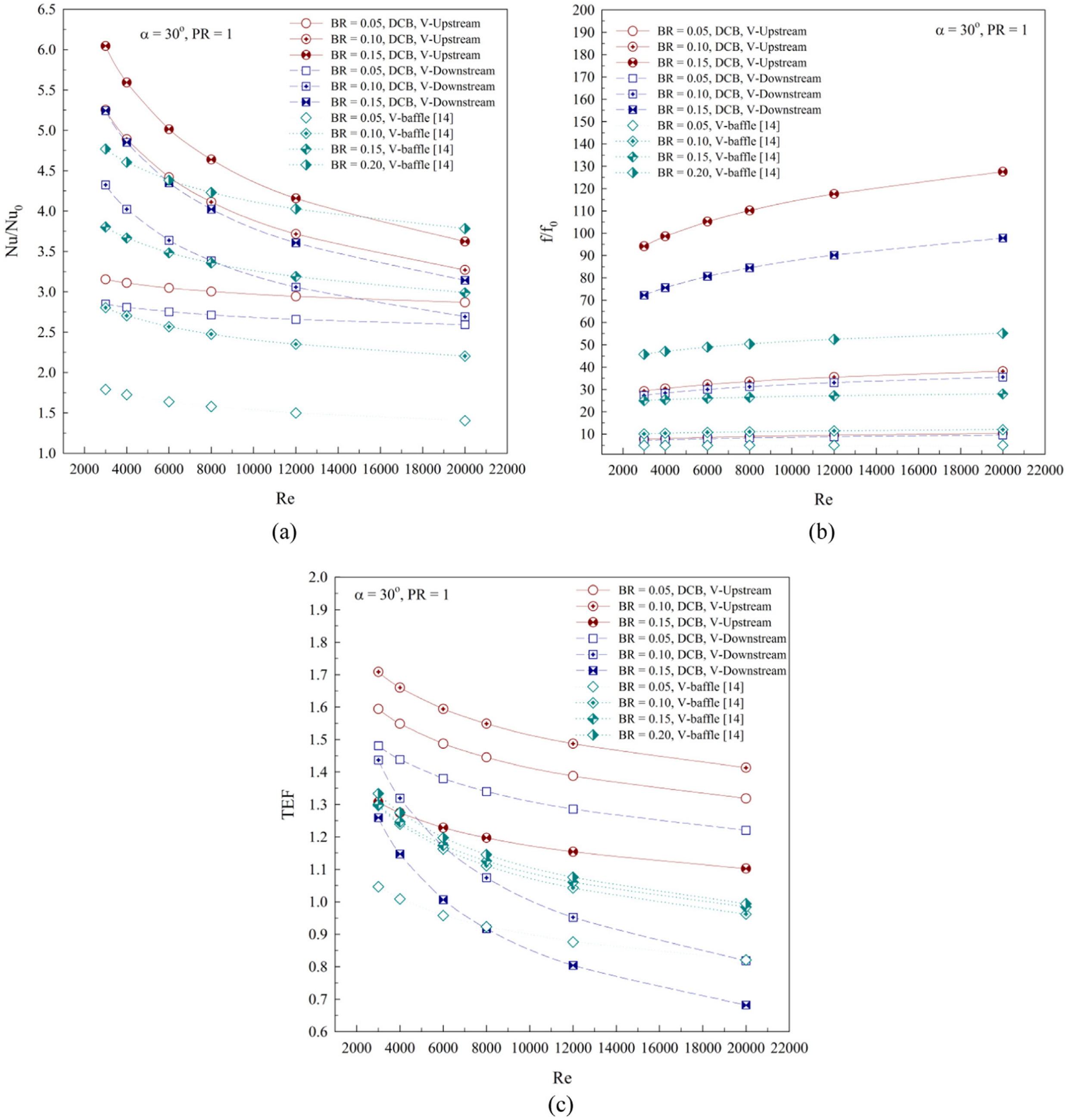

Fig. 7. Variations of the (a) Nu/Nu_0, (b) f/f_0 and (c) *TEF* with the Reynolds number of the square channel with *DCB*s and comparison with the V-baffle inserted diagonally in the channel.

walls. The impinging areas (red contour) give higher heat transfer rate than the other regimes. The impingement of the fluid flow disturbs the thermal boundary layer on the wall regions that helps to improve the heat transfer rate and thermal efficiency in the channel heat exchanger. The impinging flow on the channel wall is also detected in case of V-Downstream. In conclusion, the impingement of the fluid flow is a main key for the heat transfer enhancement.

The local Nusselt number distributions on the channel walls for the V-Upstream and V-Downstream cases are reported in the Fig. 6a and b, respectively, at $BR=0.1$ and $Re=3000$. As the figures, the V-Upstream performs greater Nusselt number than the V-Downstream. The reason of this may be that the V-Upstream of the *DCB* can produce stronger impinging flow than the V-Downstream.

5.3. Performance assessment

The performance assessments in the square channel heat exchanger with the *DCB* are plotted in terms of the Nusselt number ratio (Nu/Nu_0), friction factor ratio (f/f_0) and thermal enhancement factor (*TEF*). Fig. 7a presents the variations of the Nu/Nu_0 with the Reynolds number at various cases for the channel with the *DCB*. Generally, the Nu/Nu_0 tends to decrease with increasing the Reynolds number for all cases. The *DCB* in the channel heat exchanger can improve the heat transfer rate higher than the smooth channel ($Nu/Nu_0>1$). The $BR=0.15$ gives the highest heat transfer rate, while the $BR=0.05$ performs the reverse trend for both V-Upstream and V-Downstream cases. The V-Upstream provides higher heat transfer rate than the V-Downstream around 13%, 17.31% and 12.5% for $BR=0.15$, 0.1 and 0.05, respectively. The maximum Nusselt number is around 6, 5.2 and 3.2 times higher than the smooth channel for $BR=0.15$, 0.10 and 0.05, respectively, for V-Upstream case, while around 5.2, 4.3 and 2.8 times for V-Downstream. In range studied, the Nu/Nu_0 is found around 2.8–6.0.

Fig. 7*b* illustrates the variations of the f/f_0 with the Reynolds number at various *BR*s and flow directions. In general, the f/f_0 increases with raising the Reynolds number. The highest friction loss is detected at $BR=0.15$, while the $BR=0.05$ performs the lowest values. The V-Upstream provides higher friction loss than the V-Downstream. The friction factor is around 7.65–127.55 and 7.12–97.82 times above the smooth square channel for the V-Upstream and V-Downstream, respectively. Additionally, the V-Downstream with low *BR* can reduce the pressure loss in the channel heat exchanger.

Fig. 7*c* reports the variations of the *TEF* with the Reynolds number at various cases. In general, the *TEF* tends to decrease with augmenting the Reynolds number. The optimum *TEF* is around 1.72, 1.6 and 1.3, respectively, for $BR=0.10$, 0.05 and 0.15, for V-Upstream case. The V-Downstream gives the maximum *TEF* around 1.5, 1.42 and 1.28 for $BR=0.05$, 0.10 and 0.15, respectively, at $Re=3000$. Although, the $BR=0.15$ yields the highest heat transfer rate, but also offers very large pressure loss, therefore, lowest *TEF* is detected for both V-Downstream and V-Upstream cases.

In comparison, the *DCB* performs higher *TEF* than the V-baffle [14]. The optimum *TEF* for the V-baffle is around 1.34, while around 1.72 for the *DCB*. The V-Upstream of the *DCB* also provides upper *TEF* than the full and discrete inclined baffles [17].

6. Conclusion

The numerical investigations on heat transfer, pressure loss and thermal enhancement factor in the square channel heat exchanger with the *DCB* are performed. The influences of the blockage ratios ($BR=0.05$, 0.10 and 0.15) and flow directions (V-Upstream and V-Downstream) are studied for the turbulent flow, $Re=5000$–20,000, and also compared with the previous results. The conclusions from the current investigation are as follows;.

The disturbance of the thermal boundary layer is found when inserted *DCB* in the heating section, that helps to improve thermo-hydraulic performance.

The strengths of the vortex flow and impinging flow increase when increasing *BR*. In the range investigates, the enhancements are around 2.8–6 and 7.12–127.55 times over the smooth channel for the Nusselt number and friction factor, respectively, depended on *BR*, *Re* and flow direction. The optimum *TEF* is around 1.72 for $BR=0.10$, $Re=3000$, V-Upstream.

Acknowledgement

The authors would like to thank Assoc. Prof. Dr. Pongjet Promvonge, KMITL for suggestions. This research was funded by College of Industrial Technology, King Mongkut's University of Technology North Bangkok (Grant No. Res CIT0203/2016).

References

[1] W. Jedsadaratanachai, N. Jayranaiwachira, P. Promvonge, 3D numerical study on flow structure and heat transfer in a circular tube with V-baffles, Chin. J. Chem. Eng. 23 (2) (2015) 342–349.
[2] T. Rajaseenivasan, S. Srinivasan, K. Srithar, Comprehensive study on solar air heater with circular and V-type turbulators attached on absorber plate, Energy 88 (2015) 863–873.
[3] W. Noothong, S. Suwannapan, C. Thianpong, P. Promvonge, Enhanced heat transfer in a heat exchanger square-duct with discrete V-finned tape inserts, Chin. J. Chem. Eng. 23 (3) (2015) 490–498.
[4] P. Promvonge, Thermal performance in square-duct heat exchanger with quadruple V-finned twisted tapes, Appl. Therm. Eng. 91 (2015) 298–307.
[5] W. Jedsadaratanachai, A. Boonloi, Effects of blockage ratio and pitch ratio on thermal performance in a square channel with 30° double V-baffles, Case Stud. Therm. Eng. 4 (2014) 118–128.
[6] T. Alam, R.P. Saini, J.S. Saini, Effect of circularity of perforation holes in V-shaped blockages on heat transfer and friction characteristics of rectangular solar air heater duct, Energy Convers. Manag. 86 (2014) 952–963.
[7] T. Alam, R.P. Saini, J.S. Saini, Experimental investigation on heat transfer enhancement due to V-shaped perforated blocks in a rectangular duct of solar air heater, Energy Convers. Manag. 81 (2014) 374–383.
[8] R. Karwa, G. Chitoshiya, Performance study of solar air heater having v-down discrete ribs on absorber plate, Energy 55 (2013) 939–955.
[9] P. Promvonge, W. Jedsadaratanachai, S. Kwankaomeng, C. Thianpong, 3D simulation of laminar flow and heat transfer in V-baffled square channel, Int. Commun. Heat. Mass. Transf. 39 (1) (2012) 85–93.
[10] P. Promvonge, W. Changcharoen, S. Kwankaomeng, C. Thianpong, Numerical heat transfer study of turbulent square-duct flow through inline V-shaped discrete ribs, Int. Commun. Heat. Mass. Transf. 38 (10) (2011) 1392–1399.

[11] P. Promvonge, S. Kwankaomeng, Periodic laminar flow and heat transfer in a channel with 45° staggered V-baffles, Int. Commun. Heat. Mass. Transf. 37 (7) (2010) 841–849.
[12] P. Promvonge, Heat transfer and pressure drop in a channel with multiple 60° V-baffles, Int. Commun. Heat. Mass. Transf. 37 (7) (2010) 835–840.
[13] D.H. Lee, D.H. Rhee, K.M. Kim, H.H. Cho, H.K. Moon, Detailed measurement of heat/mass transfer with continuous and multiple V-shaped ribs in rectangular channel, Energy 34 (11) (2009) 1770–1778.
[14] W. Jedsadaratanachai, A. Boonloi, P. Promthaisong, P. Promvonge, Numerical investigation of turbulent heat transfer in a square duct with diagonal V-baffles, in: Proceedings of the 1st International Conference on Engineering Science and Innovative Technology (ESIT 2014), Krabi, Thailand, April 8–10, 2014.
[15] A. Boonloi, Thermal performance improvement in square duct with inclined ribs inserted diagonally, Asian J. Appl. Sci. 03 (02) .
[16] A. Boonloi, W. Jedsadaratanachai, Forced convection heat transfer, flow configuration and thermal performance in a sqaure channel with modified V-shaped baffles, J. Math. Stat. 10 (02) (2014) 201–210.
[17] J. Wongpueng, Numerical investigation of flow characteristics an heat transfer in square duct with angled ribs, KMITL-2014-EN-M (2014) 030–205.
[18] S.V. Patankar, Numerical Heat Transfer and Fluid Flow, Mcgraw-Hill,, 1980.
[19] P. Promvonge, S. Skullong, S. Kwankaomeng, C. Thiangpong, Heat transfer in square duct fitted diagonally with angle-finned tape—Part 2: numerical study, Int. Commun. Heat. Mass. Transf. 39 (5) (2012) 625–633.